Journals of Gerontology: Biological Sciences
cite as: J Gerontol A Biol Sci Med Sci, 2018, Vol. 74, No. 6, 760–769
doi:10.1093/gerona/gly161
Advance Access publication July 13, 2018

Editor's choice

Original Article

The Impact of Aging, Calorie Restriction and Dietary Fat on Autophagy Markers and Mitochondrial Ultrastructure and Dynamics in Mouse Skeletal Muscle

Elena Gutiérrez-Casado, BS,[1,†] Husam Khraiwesh, PhD,[2,†] José A. López-Domínguez, PhD,[1,3] Jesús Montero-Guisado, BS,[1,4] Guillermo López-Lluch, PhD,[5] Plácido Navas, PhD,[5] Rafael de Cabo, PhD,[6] Jon J. Ramsey, PhD,[7] José A. González-Reyes, PhD,[1,*] and José M. Villalba, PhD[1,*]

[1]Departamento de Biología Celular, Fisiología e Inmunología, Universidad de Córdoba, Campus de Excelencia Internacional Agroalimentario, ceiA3, Spain. [2]Department of Nutrition and Food Processing, Faculty of Agricultural Technology, Al-Balqa Applied University, Al-Salt, Jordan. [3]Present address: Buck Institute for Research on Aging, Novato, California. [4]Present address: Departamento de Biología Molecular, Instituto de Biomoléculas (INBIO), Universidad de Cádiz, Spain. [5]Centro Andaluz de Biología del Desarrollo, Universidad Pablo de Olavide-CSIC, CIBERER, Instituto de Salud Carlos III, Sevilla, Spain. [6]Translational Gerontology Branch, National Institute of Aging, National Institutes on Health, Baltimore, Maryland. [7]Department of Molecular Biosciences, School of Veterinary Medicine, University of California, Davis.

*These authors shared last authorship.
[†]These authors contributed equally to this work.

Address correspondence to: José A. González-Reyes, PhD, Departamento de Biología Celular, Fisiología e Inmunología, Universidad de Córdoba, Campus de Rabanales, Edificio Severo Ochoa, 3ª planta, Campus de Excelencia Internacional Agroalimentario, ceiA3, 14014 Córdoba, Spain. E-mail: bc1gorej@uco.es

Received: March 9, 2018; Editorial Decision Date: July 6, 2018

Decision Editor: Rozalyn Anderson, PhD

Abstract

Loss of skeletal muscle mass and function is a hallmark of aging. This phenomenon has been related to a dysregulation of mitochondrial function and proteostasis. Calorie restriction (CR) has been demonstrated to delay aging and preserve function until late in life, particularly in muscle. Recently, we reported the type of dietary fat plays an important role in determining life span extension with 40% CR in male mice. In these conditions, lard fed mice showed an increased longevity compared to mice fed soybean or fish oils. In this article, we analyze the effect of 40% CR on muscle mitochondrial mass, autophagy, and mitochondrial dynamics markers in mice fed these diets. In CR fed animals, lard preserved muscle fibers structure, mitochondrial ultrastructure, and fission/fusion dynamics and autophagy, not only compared to control animals, but also compared with CR mice fed soybean and fish oils as dietary fat. We focus our discussion on dietary fatty acid saturation degree as an essential predictor of life span extension in CR mice.

Keywords: Caloric restriction, Dietary fat, Mitochondria, Mice, Muscles

Aging affects all organs and tissues by inducing a functional decline. In skeletal muscle, sarcopenia (a loss of mass and functionality) is a well-recognized hallmark of aging (1). In humans, a decline in muscle mass of 3%–10% per decade after the age of 25 has been described (2). Decreased mitochondrial content and function has been considered to play an essential role in sarcopenia, however the exact mechanism by which aging affects mitochondria and vice-versa in skeletal muscle, is still a matter of debate.

Calorie restriction (CR; ie, a reduction in calorie intake without malnutrition) is considered the most robust nutritional intervention to

delay aging and its deleterious consequences (3). Thus, a reduction in calorie intake of 20%–40% of ad libitum fed animals not only prevents several diseases related to aging in a wide range of animals and humans, but also increases life span and/or health span in several species (4,5). CR has been shown to exert a protective effect against sarcopenia in both rodents (6) and nonhuman primates (7). Despite these results, the mechanisms by which CR operates are not completely clear.

Most mammalian muscles are basically composed of two different types of fibers: slow- and fast-twitch (8). Slow-twitch (red or type I) muscle fibers contract more slowly and rely on aerobic metabolism. They contain large amounts of mitochondria and myoglobin. Fast-twitch (white or type II) fibers contract more rapidly due to the presence of a faster myosin. In general, type II fibers contain fewer mitochondria and myoglobin than type I and rely on glycolysis to generate energy. Aging can differentially affect both types of fibers. For example, Proctor et al. (9) reported a decrease in size and oxidative capacity of white fibers without changes in the red ones. More recently, Nilwik et al. (10) observed that the decline in muscle mass during aging was due to the reduction in white fibers size, and Sayed et al. (11) have shown differential changes in several structural and ultrastructural parameters in both type of fibers from gastrocnemius muscle in aged mice.

Mitochondrial morphology and location also varies in the different fiber types. In white fibers, mitochondria are found mainly between the myofibrils. These are referred to as intermyofibrillar mitochondria (IMM). In addition, red fibers contain a high number of mitochondria located in the subsarcolemmal space (ie, the portion of sarcoplasma located between the plasmalemma and the more external myofibrils) and are called subsarcolemmal mitochondria (SSM). Both populations show differences concerning their physiology and ultrastructure and respond differentially to aging (11,12).

Sarcopenia has been associated with a decline in mitochondrial content and/or function resulting from unbalanced processes of fission and fusion and autophagy in aged animals. These processes are mediated by different proteins whose precise mechanisms of action are now beginning to be understood. Mitochondrial constriction and division (fission) is largely mediated by Drp1, while Mfn1, and Mfn2 conjoin the outer membranes and OPA1 facilitates the fusion of the inner membrane and cristae formation (13). Autophagy depends on many proteins. Among them, Beclin1 is involved in the control of autophagosome formation, while p62 and LC3 are necessary for cargo selection and autophagosome maturation (14). The specific form of selective mitochondrial autophagy (mitophagy) is mediated to a great extent by Pink1 and Parkin proteins (15). Most of these processes are decreased or modified in skeletal muscle with aging (12,14–17). However, the possible effects of CR and dietary fat on these mechanisms have not been extensively studied.

We have shown that dietary fat influences the fatty acid composition of the mitochondrial membranes from skeletal muscle in C57BL/6 mice following one month of 40% CR, which resulted in changes in several mitochondrial features (18). Using the same experimental design with longer periods of CR, lard as dietary fat exerted an optimal effect on several parameters related to mitochondrial physiology and apoptotic signaling in skeletal muscle (19). More recently, it has been demonstrated that the composition of dietary fat modulates longevity of mice fed CR diets (20). Thus, animals fed a 40% CR diet with lard (high in saturated and monounsaturated fatty acids) as the primary dietary fat exhibited extended life span compared with CR animals consuming diets containing either soybean oil (high in n-6 polyunsaturated fatty acids, PUFA) or fish oil (high in n-3 PUFAs) as the primary lipid sources (20).

The aim of this work is to ascertain whether aging influences structural and ultrastructural parameters of red fibers from mouse *gastrocnemius* with special attention to mitochondria and autophagy. We also analyzed the impact of aging, CR and dietary fat on the expression pattern of several proteins related to mitochondrial physiology (mitochondrial complexes), fission and fusion markers (Drp1, Mfn1, Mfn2, and OPA1), and auto- and mitophagy-related proteins (Beclin1, p62, LC3, Pink1, and Parkin) in hind limb skeletal muscle to determine their possible effect on sarcopenia and therefore in life and health span in rodents.

Material and Methods

Animals and Diets

We used the same cohort of male 10-week-old C57BL/6 mice (Charles River Laboratories, Spain) as in our previous publications (19–22). Animals were separated in four dietary groups: one control and three CR dietary groups that differed in lipid sources: lard, soybean oil (also for control group), and fish oil. At the end of the corresponding intervention period, the animals were euthanized by cervical dislocation after an 18-hour fast to ensure that all animals were studied in a similar metabolic state (fasted). Muscle from the hind limb was dissected, washed, and trimmed of connective tissue and fat, frozen by immersion in liquid nitrogen in a buffered medium containing 10% dimethyl sulfoxide (DMSO) as cryoprotectant, and then stored at −80°C for later analysis. Handling of animals and all experimental procedures were in accordance with the Pablo de Olavide University ethical committee rules, and the 86/609/EEC directive on the protection of animals used for experimental and other scientific purposes. In this work, we have used the characters C, L, S, and F to identify Control-Soybean oil, CR-*L*ard, CR-*S*oybean oil, and CR-*F*ish oil-fed animals, respectively, followed by 6 or 18 to denote the duration of dietary intervention (in months). Detailed procedures regarding animal experimentation and diets are described in Supplementary Methods.

Isolation of Total Homogenate Fraction from Skeletal Muscle

Hind limb skeletal muscles from four to seven animals per group were homogenized at 4°C in ice-cold buffer containing 20 mM Tris–HCl pH 7.6, 40 mM KCl, 0.2 M sucrose, 1 mM phenylmethylsulfonyl fluoride, 10 mM ethylene-diamine-tetra-acetic acid (EDTA), and 20 µg/µL each chymostatin, leupeptin, antipain, and pepstatin A in a Teflon glass tissue homogenizer. A second homogenization step was carried out using an electric tissue disrupter (Ultra-Turrax T25, IKA, Staufen, Germany) for 30 seconds. The resultant lysate, total homogenate, was used for determinations of protein levels.

Structural and Ultrastructural Analysis of Skeletal Muscle Fibers, Mitochondria, and Autophagic Figures

Samples from deep zones of the gastrocnemius (red gastrocnemius) from four to seven animals per diet and CR period were fixed and processed for electron microscopy. Semithick (0.5–1 µm width) and thin (40–60 nm width) sections were obtained and photographed in a light (Leica) and electron microscope (Jeol Jem 1400), respectively, at the Servicio Centralizado de Ayuda a la Investigación (SCAI; Univ. Córdoba, Spain). From this material we measured white and red fiber cross-sectional areas (CSA) and different parameters

including mitochondrial content, SSM spreading below sarcolemma and morphometric characteristics of mitochondria and autophagic figures in cross-sectioned red fibers using Image J software (NIH; USA). Detailed descriptions of these methods are included in the Supplementary Methods section and Supplementary Table 1.

Measurement of Mitochondrial Mass and Dynamics, Autophagy, and Mitophagy Markers

Detailed procedures are described in the Supplementary Methods. As mitochondrial mass and function markers, we used monoclonal sera raised against different subunits of mitochondrial complexes. For detection of autophagy and mitophagy markers, we used monoclonal and polyclonal sera raised against p62, LC3-I/II, Beclin1, Pink1, and Parkin at optimized concentrations (see Supplementary Table 2). Mitochondrial fusion and fission proteins were immunodetected using Mfn1, Mfn2, OPA1, and Drp1 primary antibodies at the indicated concentrations (see Supplementary Table 2). The corresponding secondary IgG antibodies coupled to horseradish peroxidase were used to reveal binding sites by enhanced chemiluminescence (Clarity TM ECL, Bio-Rad). Images obtained were analyzed using the Image Lab TM Software (Bio-Rad) and normalized to Ponceau´s staining as previously validated by our group (23). To obtain an accurate estimation of changes produced by CR per se and by alterations of dietary fat in CR animals, the effects of these two dietary manipulations were assessed in separate electrophoresis gels and blots carried out under optimized conditions for each case. Thus, these results were also represented in separate plots for CR effects (C vs S) and for dietary fat effects in CR animals (L, S, and F).

Statistical Analysis

All values are expressed as mean ± SEM. Variables were tested for normality by using D'Agostino–Pearson test. Differences between control and CR groups within a given age were assessed by two-tailed Student's *t* test. In case data did not pass the normality test, the nonparametric two-tailed Mann–Whitney test was used. The effects of dietary fat in calorie restricted animals of a given age (6 or 18 months of intervention) were assessed by one-way analysis of variance followed by post hoc analysis of significant differences with Tukey's test for multiple comparisons. Post hoc analysis of linear trend was also performed to investigate putative alterations of tested parameters among CR diets ordered as L → S → F, representative of a progressive decrease of n-6/n-3 ratio in high unsaturated fatty acids (18). In case data did not pass the normality test, the nonparametric Kruskal–Wallis test was performed followed by post hoc Dunn's multiple comparison test. For all dietary groups, possible differences as a function of age were also assessed by either parametric two-tailed Student's *t* test or nonparametric two-tailed Mann–Whitney test as required. Means were considered statistically different when $p < .05$. All statistical analyses were performed using GraphPad Prism 5.03 (GraphPad Software Inc., San Diego, CA).

Results

Skeletal Muscle Fiber Size

To assess the effect of aging and CR on morphological features of gastrocnemius muscle, we determined possible changes in fiber size after dietary interventions. In cross-sections, red and white fibers appear as polygonal structures and can be distinguished after staining of semi thick sections with toluidine blue or *p*-phenylene-diamine. Using either of these techniques, presence of SSM in red fibers is revealed by large blue or dark-brown spots detected in peripheral regions of the cells confirmed by electron microscopy (see below). More discrete dots were also found scattered in internal zones of the fibers and reveal the presence of IMM (see Supplementary Figure 1). For the present work, we have considered red fibers as those showing large numbers of colored spots below the plasmalemma, and white fibers as those lacking these stain deposits.

The analysis of both fiber types indicated a smaller size of red fibers compared to white regardless of the dietary intervention or animal age. In red fibers, aging did not alter CSA in controls, but a significant decrease was found in CR (S group) mice (Figure 1A). In white fibers, aging resulted in a significant reduction of CSA in both controls (C) and CR groups (Figure 1B).

Dietary fat differentially affected CSA of both fiber types in CR mice. In F groups (ie, CR mice with fish oil as dietary fat) a similar pattern of decreased CSA with aging was found in both fibers (Figure 1A and B), whereas this parameter remained unaltered in red fibers in L groups (CR mice with lard as fat source). Although CSA of white fibers decreased with aging in all dietary groups, the reduction in L was not as pronounced as in the other CR groups. As a result, old mice of L group exhibited significantly higher CSA compared to S (CR animals fed soybean oil as dietary fat) and F groups (Figure 1B).

Estimation of Mitochondrial Mass by Transmission Electron Microscopy

In cross-sections, SSM appear as clusters of mitochondria showing circular or elliptical shape, an electron-dense matrix and a high number of cristae. On the other hand, IMM appear smaller than SSM but display a more complex and branched morphology (see Figure 2A–H). Also, it is worth noting the presence of SSM and IMM with altered structure (swollen appearance with a low number of mitochondrial cristae and very low electron-dense matrix) in all the dietary groups regardless of age (Figure 2A–H).

In control animals, aging did not induce volume density (Vv) changes in SSM. However, long-term CR (S18 group) resulted in a significant decrease of this parameter. When comparing the different dietary groups, S18 mice showed significantly less SSM Vv compared with L18 (Figure 1C). Volume density of IMM increased significantly from 6 to 18 months in control mice, and this effect was also found in the S group (see Figure 1D). When comparing CR groups, Vv also increased with aging in L, but no change was observed in the F group (Figure 1D).

Aging, CR, Dietary Fat, and Skeletal Muscle Mitochondrial Morphology

In control animals, aging decreased SSM area (Figure 1E). Six months of CR also induced a decreased SSM area in the S group, although a recovery was observed after 18 months. Thus, no differences were found in this parameter after 18 months of intervention when comparing the C versus S groups (Figure 1E). When analyzing the effects of different dietary fats in CR mice, we found a marked increase for this parameter in L (lard) group in comparison to age-matched S and F animals. Furthermore, a decreasing linear trend for SSM area was found in both 6 and 18 months of CR ordered as L > S > F (Figure 1E).

IMM area did not change with aging in control mice but substantially increased in the S group (Figure 1F). When we compared the effect of dietary fat within a given age, the most remarkable effect was the increase of IMM area in the L group, with a significant decreasing linear trend after 18 months ordered as L18 > S18 > F18 (Figure 1F).

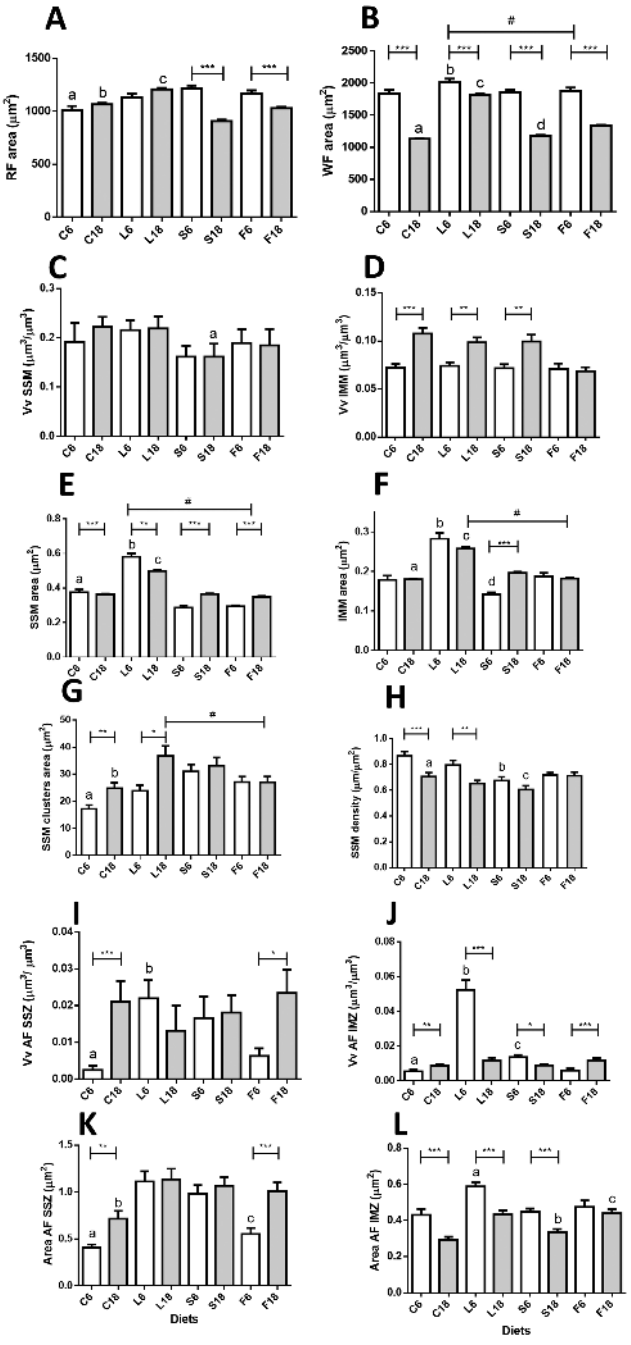

Figure 1. Morphometric characteristics of muscle fibers, mitochondria and autophagic figures from gastrocnemius muscle in control and calorie restriction (CR) mice after 6 and 18 months of intervention with different dietary fats. Panels **A** and **B** show cross-sectional area (CSA) of red and white fibers, respectively. In Panel **B**, # denotes a decreased linear trend ordered as L6 > S6 > F6. Panels **C** and **D** show Volume density (Vv) of subsarcolemmal (SSM) and intermyofibrillar mitochondria (IMM) per cell volume unit. Panels **E** and **F** show SSM and IMM areas. In Panel **E**, # denotes a significant decreasing linear trend ordered as L > S > F in CR mice after 6 and 18 months of intervention. In panel **F**, # represents a decreasing linear trend (L > S> F) at 18 months of CR. Panels **G** and **H** show mean area of SSM clusters and SSM cluster size in relation to plasmalemmal length (SSM density), respectively. In panel **G**, # represents a decreasing linear trend in 18-month CR-mice (L > S > F). Panels **I** and **J** show Vv of autophagic figures (AF) in subsarcolemmal (SSZ) and in intermyofibrillar zones (IMZ). Mean area of AF in both zones are depicted in panels **K** and **L**, respectively. In all graphs, * = $p < .05$; ** = $p < .01$, and *** = $p < .001$. Panel **A**: a = *** vs S6; b = *** vs S18; c = *** vs S18 and F18. Panel **B**: a = * vs S18; b = * vs S6; c = *** vs S18 and F18; d = *** vs F18. Panel **C**: a = * vs C18 and L18. Panel **E**: a = * vs S6; b = * vs S6 and F6; c = * vs S18 and F18. Panel **F**: a = *** vs S18; b = *** vs S6 and ** vs F6; c = *** vs S18 and F18; d = *** vs F6. Panel **G**: a = *** vs S6; b = * vs S18. Panel **H**: a = * vs S18; b = *** vs C6 and * vs L6; c = * vs F18. Panel **I**: a = * vs S6; b = * vs F6. Panel **J**: a = *** vs S6; b = *** vs S6 and F6; c = *** vs F6. Panel **K**: a = *** vs S6; b = *** vs S18; c = ** vs L6 and *** vs S6. Panel **L**: a = *** vs S6 and * vs F6; b = ** vs L18 and * vs C18; c = ** vs S18.

We also studied parameters relevant to mitochondrial subpopulations to investigate possible changes in their distribution in red fibers. As depicted in Figure 1G, the size of SSM clusters significantly increased during aging in control mice. Although 6 months of CR (S group) also resulted in a significant increase in this parameter, no further increase was induced by aging in S group. When studying the effect of aging in the different CR groups, the most noticeable effect was the age-dependent increase of SSM clusters area in L18 compared to the L6 group (Figure 1G). A decreasing linear trend for SMM clusters area was found as L18 > S18 > F18 (Figure 1G).

When analyzing the relationship between SSM clusters size and the length of sarcolemma associated with them (SSM density), we found significant decreased values during aging in controls whereas no change was observed in the S group (Figure 1H). When comparing the groups fed CR diets, no changes were observed in F mice, but a significant decrease was found in L18 versus L6 mice (Figure 1H).

Ultrastructural Analysis of Autophagy in Skeletal Muscle Fibers

Autophagic figures and altered mitochondria were observed in all the experimental groups (see Supplementary Figure 2). Volume density (Vv) of these figures in the subsarcolemmal space is shown in Figure 1I. This parameter was dramatically increased with aging in control, but not in CR animals (S group). When comparing CR groups, a decreased Vv was found in F6 compared to L6, and a marked increase of Vv with aging was observed in CR-mice with fish oil as fat source (F18 group; see Figure 1I). No significant change in Vv was observed with aging in the L group. In the intermyofibrillar spaces, Vv of autophagic figures and altered mitochondria increased with aging in controls (Figure 1J) and 6 months of CR (S group) also induced an increase in this parameter, although Vv of autophagic figures was again decreased after 18 months in such a way that no difference was observed between C18 and S18 groups. When comparing the different CR-groups, we observed a drastically increased volume density (Vv) of autophagy figures in L6 followed by a significant drop in L18. In CR animals, the only group that showed age-dependent increase of autophagic figures abundance was F, which exhibited a nearly identical pattern to that observed for controls (Figure 1J).

Mean size of autophagic figures varied depending on their position within the cell (Figure 1K and L). In subsarcolemmal zones from control mice, this parameter increased with age. In 6-month calorie-restricted animals (S6 group), autophagic figure size increased when compared to controls, but no further change was detected with aging. When comparing the different dietary fats in CR-mice, soybean and lard groups (S and L) showed no age-related changes, while changes in CR-fish oil group (F) were like those observed in controls (Figure 1K). In the intermyofibrillar zones, we observed a uniform pattern of decreasing size of autophagic figures with age in both C and S groups (Figure 1L). In CR groups, autophagic figures decreased with age in L and S groups while no age-related change

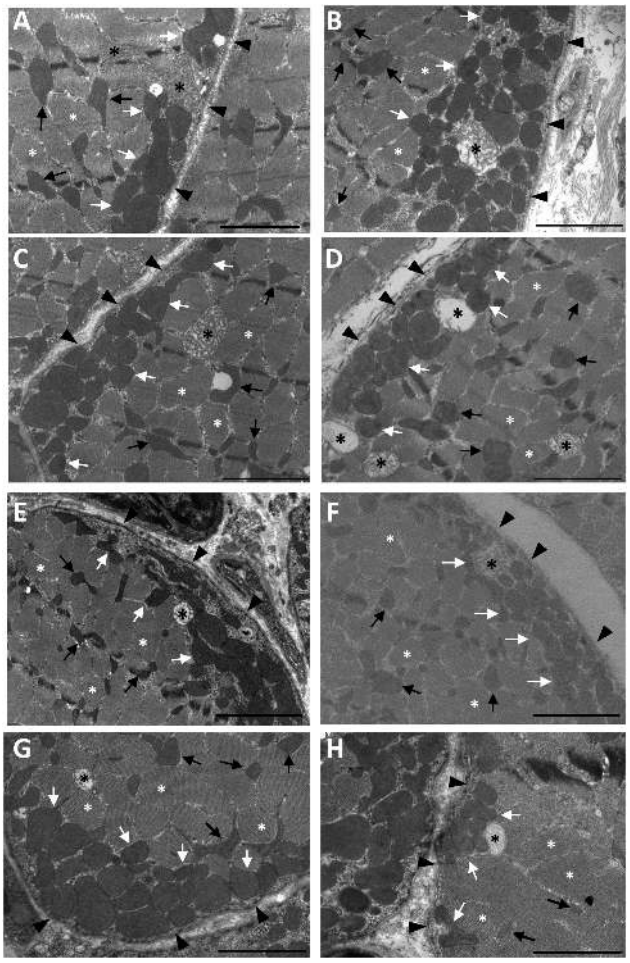

Figure 2. Examples of red fibers from mouse gastrocnemius muscle in cross-section as observed by electron microscopy. Subsarcolemmal mitochondria (SSM, white arrows) are located between the plasmalemma (black arrowheads) and myofibrils (white asterisks), while intermyofibrillar mitochondria (IMM; black arrows) are found in the sarcoplasm between the myofibrils. (**A**) C6; (**B**) L6; (**C**) S6; (**D**) F6; (**E**) C18; (**F**) L18; (**G**) S18, and (**H**) F18. Mitochondria with altered morphology are marked with black asterisks. The bars are equal to 2 μm.

was observed in F mice. Of note, the mean size of autophagic figures was significantly higher than that of mitochondria with unaltered structure, regardless of their position within the cell (compare values depicted in Figure 1E and F with those in Figure 1K and L).

Mitochondrial Complexes

In Figure 3A–J, we show the expression levels of mitochondrial complexes. In controls, aging only affected the expression level of complex I, which decreased in old animals (Figure 3A). However, in S groups, aging resulted in decreased expression of complex III (Figure 3E). Some changes among CR groups were noted after 6 months of intervention, with a general trend towards an increase of some mitochondrial complexes in animals fed PUFA-containing diets (S and F groups). Accordingly, complex II increased in F6 in comparison with L6 (Figure 3D), complex III increased in both S6 and F6 compared to L6 (Figure 3F), and complex IV increased in F6 compared to S6 (Figure 3H). However, 18 months of intervention abated these changes and no significant differences were found in these CR mice (see Figure 3B,D,F,H,J).

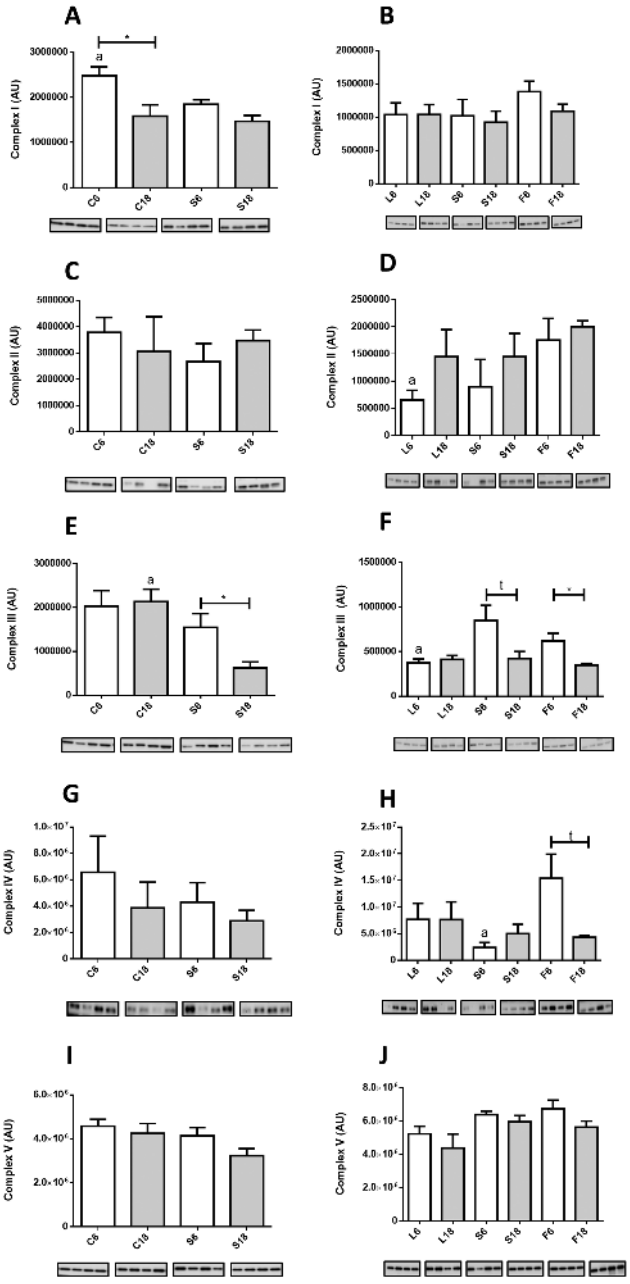

Figure 3. Expression levels of mitochondrial complexes measured by western blots from hind limb homogenates. **A** and **B**, Complex I; **C** and **D**, Complex II; **E** and **F**, Complex III; **G** and **H**, Complex IV; and **I** and **J**, Complex V. Panel **A**: a = * vs S6. Panel **D**: a = * vs F6. Panel **E**: a = *** vs S18. Panel **F**: a = * vs S6 and F6. Panel **H**: a = * vs F6.

Autophagy and Mitophagy Markers

Aging resulted in increased levels of Beclin1 in control mice (Figure 4A). The level of this protein was not significantly altered in S6 compared with C6 and no further changes were noted in S18 (Figure 4A) nor among the three CR groups fed diets with different dietary fat (Figure 4B), suggesting the existence of sustained levels of Beclin1 with aging in CR mice. For LC3-II/LC3-II+I ratio, a marker of autophagic flux, a general increasing trend with age was found in all dietary groups, although statistical significance was only obtained in the case of S and F groups (Figure 4C and D). Finally, p62 dramatically increased in controls after 18 months of

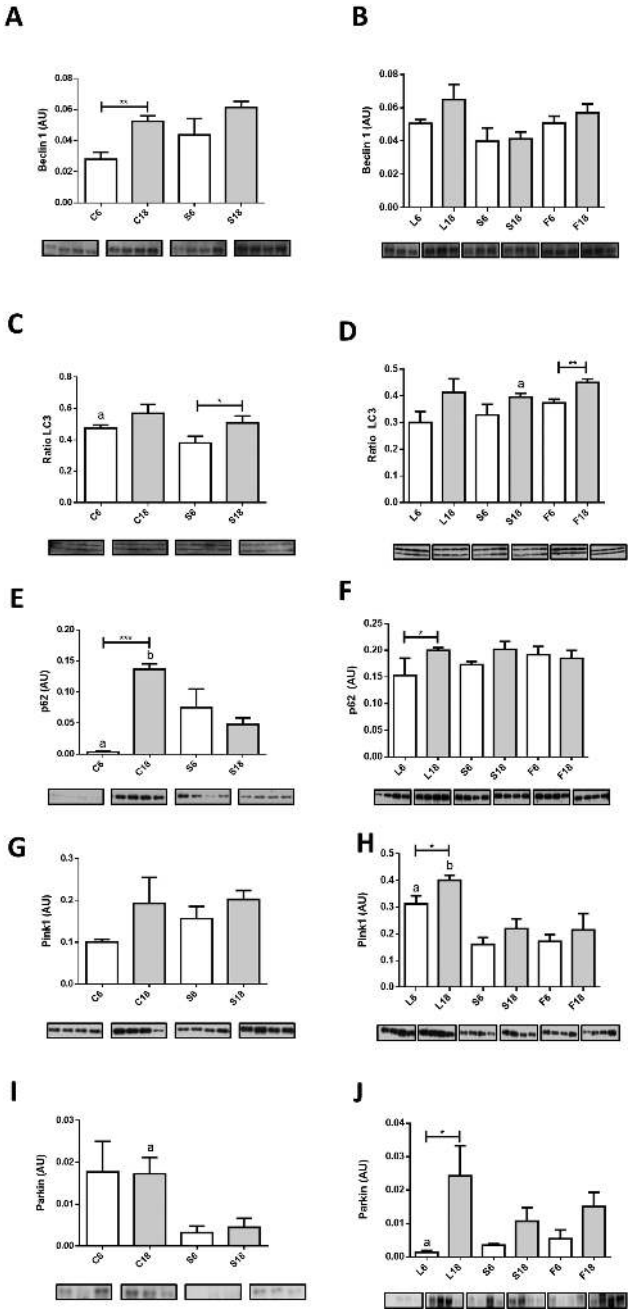

Figure 4. Expression levels of proteins related to autophagy in control and calorie restriction (CR)-mice after 6 or 18 months of intervention. **A** and **B**, Beclin1; **C** and **D**, LC3-II/LC3-I+LC3-II ratio; and **E** and **F**, p62. Protein expression levels of mitophagy markers are depicted in panels **G** and **H** (Pink1) and in **I** and **J** (Parkin). Panel **C**: a = * vs S6. Panel **D**: a = * vs F18. Panel **E**: a = * vs S6; b = *** vs S18. Panel **H**: a = ** vs S6 and * vs F6; b = ** vs S18 and * vs F18. Panel **I**: a = * vs S18. Panel **J**: a = * vs S6.

intervention (Figure 4E). However, we also found an increase of p62 levels when comparing S6 with C6, without any further change in S18 (Figure 4E). The levels of p62 were mostly unchanged when comparing the groups fed CR diets containing different dietary fats, either after 6 or 18 months of intervention, with the sole exception being an increase in L18 in comparison with L6 (Figure 4F).

In relation to mitophagy, a trend towards increased Pink1 levels with aging was found in control animals, although differences did not reach statistical significance (Figure 4G), and the same was found for S group (Figure 4H). However, when the three CR dietary groups were analyzed, it was found that levels of Pink1 increased in L18 compared to L6, whereas no change with age was observed in the F groups. Furthermore, when comparing the different CR groups at each duration of intervention, the highest levels of Pink1 were found in L6 and L18 (Figure 4H). In the case of Parkin, no effect of age was found in the control groups, but levels of this protein were significantly decreased both in S6 and S18 groups in comparison with their age-matched controls (Figure 4I). Interestingly, levels of Parkin were affected by dietary fat in CR mice, with CR-lard (L) group exhibiting significant age-dependent increase of this protein (Figure 4J).

Mitochondrial Dynamics Markers

Aging and dietary interventions affected several markers of mitochondrial fusion/fission. No changes in Mfn1 levels were observed in control and soybean oil CR mice (C and S groups, respectively) and modifying dietary fat in animals fed a CR diet did not alter the levels of this protein (Figure 5A and B). Nevertheless, Mfn2 levels increased significantly in C18 versus C6 and a similar trend was observed when comparing S6 and S18, although in this case differences did not reach statistical significance (Figure 5C). Mfn2 levels were also increased in S6 compared with C6, but no differences were observed between S18 and C18. Furthermore, no differences were found when comparing the different dietary fats in CR mice, either after 6 or 18 months of intervention (Figure 5D). OPA1 levels were not affected by aging in control mice, and CR significantly increased OPA1 levels in young (S6) but not in old (S18) mice (Figure 5E). Although OPA1 levels remained unaltered with aging in S groups, a significant increase after 18 months of CR was observed both in L and F groups (Figure 5F). A linear trend was also found in these groups when ordered as L18 > S18 > F18 (Figure 5F).

In control animals, aging had no effect on the expression levels of the fission-related protein Drp1 although an increase was found in S18 versus C18 groups (Figure 5G). However, no effect of age or dietary fat was found when comparing the CR groups (Figure 5H).

Discussion

Aging, CR, and Fiber Size

In different mammalian models, aging results in reduced CSA in white fibers without significant changes in red ones (24,25), a situation that is delayed by CR (6,25,26). In accordance with these reports, we found decreased CSA during aging in white fibers from control and CR mice regardless the dietary fat. However, in animals fed lard as dietary fat (L groups), the reduction in CSA with age was considerably less compared to the other CR groups. Aging did not result in decreased CSA of red fibers in controls, but markedly decreased CSA in soybean and fish oil fed CR mice (S and F groups), an effect that was not observed in CR-lard fed animals (L groups), which maintained this parameter at similar values after 6 or 18 months of intervention. These results point out lard as a dietary fat that preserves CSA of skeletal muscle with aging in CR mice, which agrees with our previous demonstration that lard also optimized several parameters related to apoptotic signaling in skeletal muscle (19).

Mitochondrial Mass in Red Fibers

Impaired mitochondrial energetics and increased mitochondria-mediated apoptosis have been found in aged skeletal muscle (1,27).

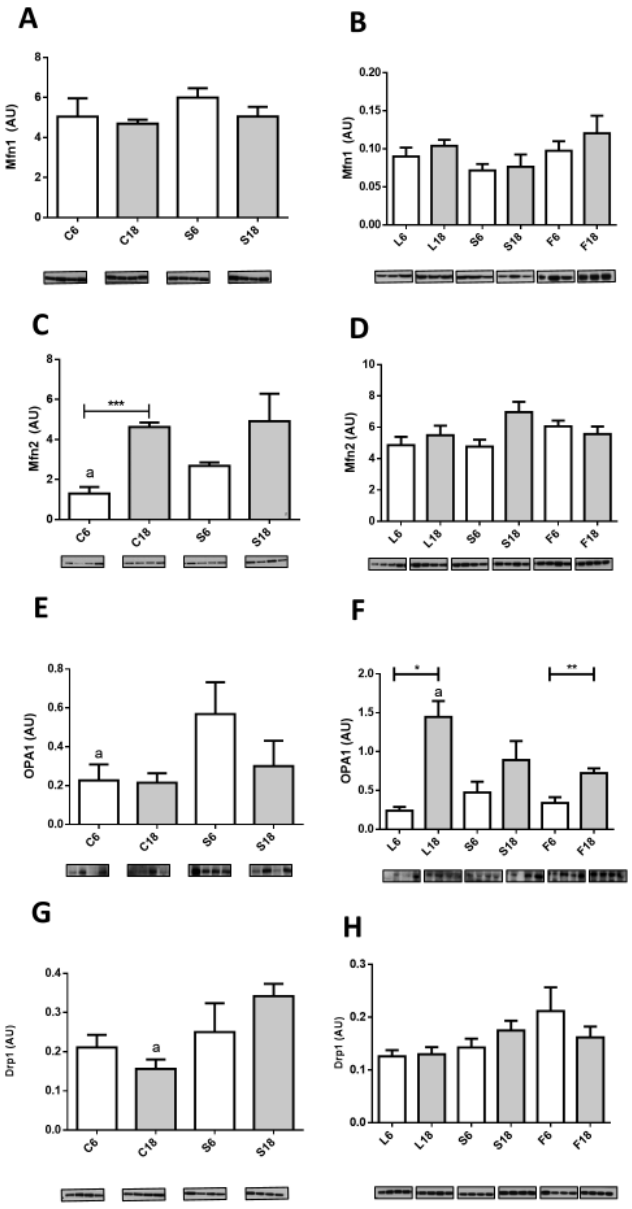

Figure 5. Expression levels of proteins related to mitochondrial fusion Mfn1 (**A** and **B**), Mfn2 (**C** and **D**), and OPA1 (**E** and **F**) and fission Drp1 (**G** and **H**) after 6 or 18 months of calorie restriction (CR) with the different fat sources. In Panel **F**, # denotes a linear trend in 18 month-CR mice ordered as L18 > S18 > F18. Panels **C** and **E**: a = * vs S6. Panel **F**: a = * vs F18. Panel **G**: a = ** vs S18.

Consequently, changes in mitochondrial content and/or ultrastructure should be expected to occur in this tissue during aging. Regarding mitochondrial mass some reported results have not been uniform. Whereas decreased mitochondrial content during aging has been reported in several species (13,28), other studies have shown that this parameter varies depending on the muscle being examined, as increased mass with aging has been found for some muscles, but decreased mass was also found for others (29,30). These differences between studies have been explained based on heterogeneity in the methods used to assess mitochondrial content (27). It is worth noting that most of the above-mentioned results were obtained by physiological and biochemical techniques using whole muscles, without reference to fiber type or to mitochondrial subpopulation. Nevertheless, in a previous analysis carried out in mice, Finley et al. (31) found that CR induced decreased mitochondrial number in white fibers without changes in red fibers.

Using electron microscopy, we found an increase in the abundance of IMM from red fibers during aging in control mice, a result that is in contrast with those reported by Leduc-Gaudet et al. (12), who found no changes in mitochondrial content in aged mice, although without discrimination between fiber types. More recently, Sayed et al. (11) found increased IMM content with aging in females from the same strain of mice used in our work. Although these latter data are in accordance with ours, no mention to fiber type was made in that paper. Of note, our results have documented that 6 months of CR induced no changes in SMM or IMM content in the S group, but longer periods of CR affected mitochondrial content in different ways depending on dietary fat. In general, CR mice showed lower mitochondrial content than controls with L18 mice displaying the highest content. As we have shown here, mitochondria with altered structure may be found in subsarcolemmal areas and intermyofibrillar regions in all the experimental groups, but they were not included in our estimation of mitochondrial mass to focus our study towards structurally intact organelles. The significance of these altered structures will be discussed below.

Using mitochondrial complexes as markers of mitochondrial mass, an age-dependent decrease was only demonstrated for Complex I, which is basically in line with previous reports (12,15). When we analyzed the effects of CR (ie, comparing C vs S groups), the only change concerning mitochondrial complexes was a decrease in Complex III after 18 months of intervention. Moreover, although 6 months of CR resulted in several changes in the expression levels of mitochondrial complexes depending on the dietary fat, including the increase of complexes II, III, and IV in mice fed diets enriched in PUFA, a longer CR intervention (18 months) abolished these changes.

Mitochondrial Ultrastructure in Red Fibers

Aging also influences morphometric parameters of individual mitochondria. Leduc-Gaudet et al. (12) found increased size of SSM as well as longer and more branched IMM in gastrocnemius from aged mice. These results contrast with those reported here since we found a slight but statistically significant decrease of sizes in SSM and no changes in IMM in control conditions during aging. However, 6 months of CR induced changes depending on the dietary fat with significantly increased size in both types of mitochondria when lard was used as dietary fat. After 18 months of CR both S18 and especially L18 showed larger mitochondria than F18. These results seem to point out a specific role of dietary fat on development of mitochondrial size and shape in CR conditions.

In skeletal muscle, it has been proposed that paravascular mitochondria (which are equivalent to subsarcolemmal) are involved in the generation of proton-motive force near the capillaries and are directly connected to a specific type of IMM called I-band mitochondria, that use the proton-motive force to produce ATP (32). Here, we show that SSM regions from old control mice are larger than those from their CR counterparts. This may be an age-related adaptive change that produces the advantage of higher contact surface of SSM clusters with IMM, which facilitates the formation of contact between them. In CR mice, only those fed lard as dietary fat showed this possible advantage.

Autophagy, Mitophagy, Aging, and CR

Results showing impaired autophagy during aging in skeletal muscle have been reported (14,15,17). In our ultrastructural

study in red fibers, we found typical autophagosomes and a relatively high number of altered mitochondria depending on the age and dietary intervention. While autophagosomes were mainly located in subsarcolemmal areas, altered mitochondria were found throughout the sarcoplasm. In general, these structures displayed greater size than nonaltered mitochondria and the possibility exists that their increased size make them unsuitable to be removed by the autophagosome leading to their accumulation inside the fibers, a mechanism previously proposed to explain increased mitochondrial size without changes in mitophagy in muscle fibers from different mammals (15). The possibility of an upper size limit for individual autophagosomes has been previously suggested (33).

In rats, Wohlgemuth et al. (17) reported increased Beclin1 expression in older animals without changes in the LC3-II to LC3-I ratio, a marker of autophagic flux, consistent with the results reported here for control animals. However, other studies in mice (34) showed decreased levels of Beclin-1 with no changes in LC3 ratio during aging. Nevertheless, these authors also found significantly increased levels of p62 expression (which is associated with a blockade in autophagic activity), suggesting a decrease in autophagic flux during aging. Except for Beclin1 changes reported by Joseph et al. (34), the results taken together are in accordance with our finding for control animals.

In our samples, 6 or 18 months of CR induced no changes in Beclin1 expression levels as occurred in CR rats (17). Although some changes were detected after 6 months of CR for LC3 ratio compared to control mice, longer periods of intervention reverted this effect. On the other hand, 18 months of CR resulted in decreased levels of p62 when compared to control, suggesting a possible unblocking of the autophagy flux. When comparing the different dietary fats, the main detected change was an age-related increase of LC3 ratio in mice fed a diet containing fish oil. This result may be related to an improvement of the autophagic flux in later age in this dietary group.

Pink1 and Parkin are directly related to selective mitophagy. In our samples, we did not find changes in the levels of these proteins during aging in controls, which agrees with previous observations in aged mice and monkeys (15). Recently, it has been reported that Pink1 is imported to mitochondria and either targeted to inner mitochondrial membranes in "healthy" mitochondria (ie, those showing a polarized membrane potential) to regulate mitochondrial bioenergetics or retained on the outer membrane in depolarized organelles (35). In the latter case, Pink1 can interact with Parkin triggering mitophagy (35). In our samples, 6 months of CR resulted in decreased levels of Parkin with no changes in Pink1, especially in mice fed lard as dietary fat and these animals showed the highest accumulation of altered IMM at this time point. After 18 months of CR, the highest values of Pink1 and Parkin were found in lard group, in which we found increased size of unaltered mitochondrial. These results seem to indicate that the relative amounts of these proteins can determine the function of Pink1 and mitochondrial fate.

Mitochondrial Fusion/Fission Markers

The analysis of mitochondrial fusion regulation in relation to aging has yielded contrasting results with a downregulated pattern found in some cases (16) and no changes or even upregulation in others (34). In a recent study carried out on mice, it has been shown that aging does not alter the expression levels of proteins related to mitochondrial fission or fusion but an increased Mfn2/Drp1 ratio was found (12). The suggestion was made that these results are compatible with a fusion–fission imbalance in favor of enhanced mitochondrial fusion in aged skeletal muscle (12). Although we did not find changes in Mfn1 and/or OPA1 expression levels in aged control mice, our results agree with this idea since increased Mfn2 levels were found in these animals. Furthermore, in a recent paper, increased levels of both Mfn1 and Mfn2 were reported in mice and monkeys (15).

Six months of CR induced increased levels of Mfn2 and OPA1, but no further changes were found after longer periods of CR, suggesting an early control of mitochondrial fusion in calorie restricted animals. This fact together with the higher expression level of Drp1 at 18 months of CR is probably a part of the regulatory mechanisms of mitochondrial fission and fusion dynamics in CR-mice and seems to operate in a different way that in control animals.

Concerning dietary fat in CR-fed mice, the most prominent result was the significative increase of OPA1 during aging in lard group (L18). It is known that OPA1 can be found in long and short forms depending on its cleavage once imported to the mitochondria. The long form is inserted in the inner mitochondrial membrane facing Mfn1 and Mfn2 proteins and is involved in outer membrane fusion, while the short form contributes to crista junction formation and interacts with several inner membrane components (36). In the present study, only the long form was clearly detected and quantified and, therefore, our results should be interpreted based on its interaction with Mfn1 and Mfn2 to promote mitochondrial fusion.

Concluding Remarks

We show that in skeletal muscle from CR mice, dietary fat influences mitochondrial mass and ultrastructure and may play a role in processes such as auto- and mitophagy and mitochondrial dynamics during aging, with lard showing some advantages compared to soybean and fish oil. These results are in accordance with previous papers using the same animals as those included here, in which we showed that dietary fat in CR mice differentially improved ultrastructural and physiological parameters in liver and kidney (21,22), with lard showing an optimal effect.

The oldest animals used in this work were 21-month-old reflecting late middle age, and sarcopenia is more apparent in advanced ages (28–30 months). Although we would hypothesize that all mice would show a decrease in muscle mass and strength with very advanced age, a limitation of the present study is that we were not able to determine the impact of dietary fats on muscle changes in elderly mice. However, we have shown that 40% CR extended life span in male mice to different degree depending on the dietary fat, with lard having the strongest effect on life span extension (20). Moreover, we also have recently reported that muscle strength and endurance is either not altered or improved in mice consuming mildly restricted high fat or ketogenic diets containing lard as the primary dietary fat when compared to a control group consuming a diet with soybean oil as the lipid source (37). These results strongly suggest an interplay between diet composition and CR in life span outcomes in mice.

On the other hand, we have also shown that mitochondrial phospholipid fatty acid composition was altered in liver and skeletal muscle from CR mice in a manner that reflected the unsaturated fatty acid composition of the diet, with the consequent increase of n-3 and n-6 fatty acids in fish and soybean oil fed animals, respectively, potentially changing several properties of the membranes (18). Additionally, lard fed animals showed a significantly higher proportion of mitochondrial monounsaturated fatty acids (especially oleic acid), a result that was accompanied by improved mitochondrial functions and ultrastructure (38). Thus,

it is very likely that an increase in monounsaturated fatty acids, such as oleic acid, may be involved in the beneficial effect of lard as a dietary fat in CR fed animals. However, further studies will be required to identify the specific fatty acids which influence muscle mass and function and health and life span in calorie restricted mice at very advanced age.

Supplementary Material

Supplementary data is available at *The Journals of Gerontology, Series A: Biological Sciences and Medical Sciences* online.

Funding

This study was supported by National Institutes of Health grant 1R01AG028125 (to J.J.R., P.N. and J.M.V.); Spanish Ministerio de Economía y Competitividad BFU2015-64630-R cofinanced with EU FEDER funds (to J.M.V.); Spanish Junta de Andalucía (Proyectos Internacionales grant and BIO-276 to J.M.V.; BIO-177 to P.N.); and Universidad de Córdoba. E.G.C. and J.A.L.D. were supported by FPU contracts from the Spanish Ministerio de Educación, Cultura y Deporte. H.K. was funded by the Spanish Agencia Española de Cooperación Internacional al Desarrollo. Rd.C. is supported by the Intramural Research Program of the National Institute on Aging.

Acknowledgments

The authors are indebted to the personnel from the Servicio Centralizado de Apoyo a la Investigación (SCAI; University of Córdoba) for technical support.

Conflict of Interest

None reported.

References

1. Johnson ML, Robinson MM, Nair KS. Skeletal muscle aging and the mitochondrion. *Trends Endocrinol Metab*. 2013;24:247–256. doi:10.1016/j.tem.2012.12.003
2. Nair KS. Aging muscle. *Am J Clin Nutr*. 2005;81:953–963. doi:10.1093/ajcn/81.5.953
3. Speakman JR, Mitchell SE. Caloric restriction. *Mol Aspects Med*. 2011;32:159–221. doi:10.1016/j.mam.2011.07.001
4. Colman RJ, Anderson RM, Johnson SC, et al. Caloric restriction delays disease onset and mortality in rhesus monkeys. *Science*. 2009;325:201–204. doi:10.1126/science.1173635
5. Mattison JA, Roth GS, Beasley TM, et al. Impact of caloric restriction on health and survival in rhesus monkeys from the NIA study. *Nature*. 2012;489:318–321. doi:10.1038/nature11432
6. Aspnes LE, Lee CM, Weindruch R, et al. Caloric restriction reduces fiber loss and mitochondrial abnormalities in aged rat muscle. *FASEB J*. 1979;11:573–581. doi:10.1096/fasebj.11.7.9212081
7. Colman RJ, Beasley TM, Allison DB, Weindruch R. Attenuation of sarcopenia by dietary restriction in rhesus monkeys. *J Gerontol A Biol Sci Med Sci*. 2008;63:556–559. doi:10.1093/gerona/63.6.556
8. Schiaffino S, Reggiani C. Fiber types in mammalian skeletal muscles. *Physiol Rev*. 2011;91:1447–1531. doi:10.1152/physrev.00031.2010
9. Proctor DN, Sinning WE, Walro JM, Sieck GC, Lemon PW. Oxidative capacity of human muscle fiber types: effects of age and training status. *J Appl Physiol (1985)*. 1995;78:2033–2038. doi:10.1152/jappl.1995.78.6.2033
10. Nilwik R, Snijders T, Leenders M, et al. The decline in skeletal muscle mass with aging is mainly attributed to a reduction in type II muscle fiber size. *Exp Gerontol*. 2013;48:492–498. doi:10.1016/j.exger.2013.02.012
11. Sayed RK, de Leonardis EC, Guerrero-Martínez JA, et al. Identification of morphological markers of sarcopenia at early stage of aging in skeletal muscle of mice. *Exp Gerontol*. 2016;83:22–30. doi:10.1016/j.exger.2016.07.007
12. Leduc-Gaudet JP, Picard M, St-Jean Pelletier F, et al. Mitochondrial morphology is altered in atrophied skeletal muscle of aged mice. *Oncotarget*. 2015;6:17923–17937. doi:10.18632/oncotarget.4235
13. Peterson CM, Johannsen DL, Ravussin E. Skeletal muscle mitochondria and aging: a review. *J Aging Res*. 2012;2012:194821. doi:10.1155/2012/194821
14. Rodney GG, Pal R, Abo-Zahrah R. Redox regulation of autophagy in skeletal muscle. *Free Radic Biol Med*. 2016;98:103–112. doi:10.1016/j.freeradbiomed.2016.05.010
15. Mercken EM, Capri M, Carboneau BA, et al. Conserved and species-specific molecular denominators in mammalian skeletal muscle aging. *NPJ Aging Mech Dis*. 2017;3:8. doi:10.1038/s41514-017-0009-8
16. Sebastián D, Sorianello E, Segalés J, et al. Mfn2 deficiency links age-related sarcopenia and impaired autophagy to activation of an adaptive mitophagy pathway. *EMBO J*. 2016;35:1677–1693. doi:10.15252/embj.201593084
17. Wohlgemuth SE, Seo AY, Marzetti E, Lees HA, Leeuwenburgh C. Skeletal muscle autophagy and apoptosis during aging: effects of calorie restriction and life-long exercise. *Exp Gerontol*. 2010;45:138–148. doi:10.1016/j.exger.2009.11.002
18. Chen Y, Hagopian K, McDonald RB, et al. The influence of dietary lipid composition on skeletal muscle mitochondria from mice following 1 month of calorie restriction. *J Gerontol A Biol Sci Med Sci*. 2012;67:1121–1131. doi:10.1093/gerona/gls113
19. López-Domínguez JA, Khraiwesh H, González-Reyes JA, et al. Dietary fat modifies mitochondrial and plasma membrane apoptotic signaling in skeletal muscle of calorie-restricted mice. *Age (Dordr)*. 2013;35:2027–2044. doi:10.1007/s11357-012-9492-9
20. López-Domínguez JA, Ramsey JJ, Tran D, et al. The influence of dietary fat source on life span in calorie restricted mice. *J Gerontol A Biol Sci Med Sci*. 2015;70:1181–1188. doi:10.1093/gerona/glu177
21. Khraiwesh H, López-Domínguez JA, López-Lluch G, et al. Alterations of ultrastructural and fission/fusion markers in hepatocyte mitochondria from mice following calorie restriction with different dietary fats. *J Gerontol A Biol Sci Med Sci*. 2013;68:1023–1034. doi:10.1093/gerona/glt006
22. Calvo-Rubio M, Burón MI, López-Lluch G, et al. Dietary fat composition influences glomerular and proximal convoluted tubule cell structure and autophagic processes in kidneys from calorie-restricted mice. *Aging Cell*. 2016;15:477–487. doi:10.1111/acel.12451
23. Bello RI, Alcaín FJ, Gómez-Díaz C, López-Lluch G, Navas P, Villalba JM. Hydrogen peroxide- and cell-density-regulated expression of NADH-cytochrome b5 reductase in HeLa cells. *J Bioenerg Biomembr*. 2003;35:169–179. doi:10.1023/A:1023702321148
24. Korhonen MT, Cristea A, Alén M, et al. Aging, muscle fiber type, and contractile function in sprint-trained athletes. *J Appl Physiol (1985)*. 2006;101:906–917. doi:10.1152/japplphysiol.00299.2006
25. McKiernan SH, Colman RJ, Lopez M, et al. Caloric restriction delays aging-induced cellular phenotypes in rhesus monkey skeletal muscle. *Exp Gerontol*. 2011;46:23–29. doi:10.1016/j.exger.2010.09.011
26. McKiernan SH, Colman RJ, Aiken E, et al. Cellular adaptation contributes to calorie restriction-induced preservation of skeletal muscle in aged rhesus monkeys. *Exp Gerontol*. 2012;47:229–236. doi:10.1016/j.exger.2011.12.009
27. Cartee GD, Hepple RT, Bamman MM, Zierath JR. Exercise promotes healthy aging of skeletal muscle. *Cell Metab*. 2016;23:1034–1047. doi:10.1016/j.cmet.2016.05.007
28. Leeuwenburgh C, Gurley CM, Strotman BA, Dupont-Versteegden EE. Age-related differences in apoptosis with disuse atrophy in soleus muscle. *Am J Physiol Regul Integr Comp Physiol*. 2005;288:R1288–R1296. doi:10.1152/ajpregu.00576.2004
29. Lyons CN, Mathieu-Costello O, Moyes CD. Regulation of skeletal muscle mitochondrial content during aging. *J Gerontol A Biol Sci Med Sci*. 2006;61:3–13. doi:10.1093/gerona/61.1.3
30. Picard M, Ritchie D, Thomas MM, Wright KJ, Hepple RT. Alterations in intrinsic mitochondrial function with aging are fiber type-specific and do not explain differential atrophy between muscles. *Aging Cell*. 2011;10:1047–1055. doi:10.1111/j.1474-9726.2011.00745.x

31. Finley LW, Lee J, Souza A, et al. Skeletal muscle transcriptional coactivator PGC-1α mediates mitochondrial, but not metabolic, changes during calorie restriction. *Proc Natl Acad Sci USA*. 2012;109:2931–2936. doi:10.1073/pnas.1115813109
32. Glancy B, Hartnell LM, Malide D, et al. Mitochondrial reticulum for cellular energy distribution in muscle. *Nature*. 2015;523:617–620. doi:10.1038/nature14614
33. Klionsky DJ, Abdelmohsen K, Abe A, et al. Guidelines for the use and interpretation of assays for monitoring autophagy. *Autophagy* 2016;12:1–222. doi:10.1080/15548627.2015.1100356
34. Joseph AM, Adhihetty PJ, Wawrzyniak NR, et al. Dysregulation of mitochondrial quality control processes contribute to sarcopenia in a mouse model of premature aging. *PLoS One*. 2013;8:e69327. doi:10.1371/journal.pone.0069327
35. Tsai PI, Lin CH, Hsieh CH, et al. PINK1 phosphorylates MIC60/Mitofilin to control structural plasticity of mitochondrial Crista junctions. *Mol Cell*. 2018;69:744–756.e6. doi:10.1016/j.molcel.2018.01.026
36. Del Dotto V, Mishra P, Vidoni S, et al. OPA1 isoforms in the hierarchical organization of mitochondrial functions. *Cell Rep*. 2017;19:2557–2571. doi:10.1016/j.celrep.2017.05.073
37. Roberts MN, Wallace MA, Tomilov AA, et al. A ketogenic diet extends longevity and healthspan in adult mice. *Cell Metab*. 2017;26:539–546.e5. doi:10.1016/j.cmet.2017.08.005
38. Villalba JM, López-Domínguez JA, Chen Y, et al. The influence of dietary fat source on liver and skeletal muscle mitochondrial modifications and lifespan changes in calorie-restricted mice. *Biogerontology*. 2015;16:655–670. doi:10.1007/s10522-015-9572-1